THE JOURNAL OF BIOLOGICAL CHEMISTRY
Vol. 277, No. 15, Issue of April 12, pp. 12735–12740, 2002

Printed in U.S.A.

Trichostatin A-induced Detransformation Correlates with Decreased Focal Adhesion Kinase Phosphorylation at Tyrosine 861 in *ras*-transformed Fibroblasts*

Received for publication, November 16, 2001, and in revised form, January 28, 2002
Published, JBC Papers in Press, January 30, 2002, DOI 10.1074/jbc.M111011200

Yangmi Lim‡§, Innoc Han‡, Ho Jeong Kwon¶, and Eok-Soo Oh‡‖

From the ‡Department of Life Sciences, Division of Molecular Life Sciences and Center for Cell Signaling Research, Ewha Womans University, Seoul 120-750, Korea and the ¶Department of Bioscience and Biotechnology, Institute of Bioscience, Sejong University, Seoul 143-747, Korea

To elucidate the role of focal adhesion kinase (pp125FAK) in transformation, its phosphorylation in transformed fibroblasts was compared with that of detransformed fibroblasts induced by a histone deacetylase inhibitor, trichostatin A (TSA). Inhibition of histone deacetylase activity in two different *ras*-transformed fibroblast lines by TSA induced a morphological change into a flattened and more spread morphology, implying detransformation. These morphological changes included increased spreading ability of transformed NIH 3T3 cells on fibronectin. Of the six tyrosine phosphorylation sites in pp125FAK, phosphorylation at position 861 (Tyr-861) was clearly decreased during detransformation by TSA. It resulted from decreased activity of Src family tyrosine kinase and/or decreased amount of Src kinase interacting with pp125FAK. Furthermore, phosphorylation of Tyr-861 was reduced substantially by the Src family kinase inhibitor, PP1, while overexpression of Src kinase increased its phosphorylation, implying that Src kinase regulates phosphorylation of pp125FAK at Tyr-861. All of these findings suggest that increased phosphorylation of pp125FAK at Tyr-861 correlates with Ras-induced transformation of fibroblasts, and TSA is able to detransform them through regulation of pp125FAK phosphorylation at Tyr-861 by an Src family kinase.

Altered cellular structure, shape, and cytoskeletal architecture are hallmarks of malignant transformation (1). One of the most characteristic cytoskeletal changes in tumor cells is the loss of actin stress fibers, suggesting that alteration of the actin-containing microfilament system is crucial for transformation (2). Several cytoskeletal proteins are known to be down-regulated in transformed cells (3), and overexpression of the reduced proteins can revert the transformed cell morphology into normal phenotypes (4). Thus, cytoskeletal protein regulation is intrinsic to the morphology of transformed cells.

Modification of chromatin structure by histone acetylation is an important mechanism in controlling gene transcription (5, 6). The acetylation state of histone is regulated by reversible enzymes, histone acetyltransferase and histone deacetylase (HDAC)[1] (7–9). Trichostatin A (TSA), a potent and specific inhibitor of HDAC (10, 11), is widely used to study the role of histone acetylation in gene expression. Recently, it has been shown that inhibition of HDAC activity by TSA is able to revert the morphological changes seen following the transformation of cells in culture with v-*sis* and v-*ras* oncogenes (12). TSA-treated cells become more flattened and have well organized actin stress fibers (13, 14). Therefore, TSA has an ability to detransform at least *ras*-transformed fibroblasts.

Cytoskeletal organization is primarily regulated by cell-ECM interactions (15, 16), and integrin receptors regulate these processes (16–19). Integrin-mediated signaling and the cytoskeletal organization are also intimately linked (20–22). As integrins bind to ECM, they become clustered and associate with cytoskeleton and signaling complexes that promote the assembly of actin filaments (20, 22). The reorganization of actin filaments into larger stress fibers, in turn, causes more integrin clustering, thus enhancing matrix binding and organization by integrins in a positive feedback system (22). Tyrosine phosphorylation has been shown to be a common and ubiquitous response to integrin-ECM interaction (22), and focal adhesion kinase (pp125FAK) is the major tyrosine-phosphorylated protein during cell-ECM interaction.

pp125FAK participates in the regulation of cytoskeletal organization as a cytosolic kinase, which phosphorylates cytoskeletal proteins such as paxillin (23), and/or a scaffolding protein for the recruitment of other Src homology 2 (SH2) or SH3-containing signaling molecules. Tyrosine phosphorylations of pp125FAK regulate its interactions and functions (24). Six tyrosine phosphoacceptor sites in pp125FAK have been identified, namely Tyr-397, Tyr-407, Tyr-576, Tyr-577, Tyr-861, and Tyr-925 (25, 26). Upon integrin engagement, pp125FAK is autophosphorylated on Tyr-397 (27), creating a high affinity binding site for the Src family tyrosine kinases via their SH2 domains (25, 26, 28) and/or the p85 regulatory subunit of phosphoinositol 3-kinase (29, 30). Association of c-Src leads to additional pp125FAK phosphorylation at Tyr-925 to create binding sites for SH2-containing proteins such as growth factor receptor-bound protein 2 (Grb2) (26, 31), which in turn activates the *ras* cascade pathway. Maximal catalytic activity of pp125FAK is achieved by Tyr-576 and Tyr-577 phosphorylation and Src kinase association (25). In addition, in-

* This work was supported by Ministry of Health and Welfare Grant HMP-00-B-20800-0080 and by the Korea Science and Engineering Foundation through the Center for Cell Signaling Research at Ewha Womans University. The costs of publication of this article were defrayed in part by the payment of page charges. This article must therefore be hereby marked "*advertisement*" in accordance with 18 U.S.C. Section 1734 solely to indicate this fact.

§ Supported by a fellowship from the Brain Korea 21 project.

‖ To whom correspondence should be addressed: Center for Cell Signaling Research, Ewha Womans University, Daehyun-dong, Seodaemoon-Gu, Seoul 120-750 Korea. Tel.: 82-2-3277-3761; Fax: 82-2-3277-3760; E-mail: OhES@mm.ewha.ac.kr.

[1] The abbreviations used are: HDAC, histone deacetylase; TSA, trichostatin A; ECM, extracellular matrix; FAK, focal adhesion kinase; SH2 and SH3, Src homology 2 and 3, respectively; SFM, serum-free medium; RIPA, radioimmune precipitation; FN, fibronectin.

creased phosphorylation of Tyr-407 and Tyr-861 has been found in Src-transformed cells (25), but the exact role of this phosphorylation is unclear. Since many functions of pp125FAK are dependent on tyrosine phosphorylation, the high level of pp125FAK phosphorylation may alter the normal functions of pp125FAK. This is the case in cell transformation. pp125FAK is heavily tyrosine-phosphorylated in Src-transformed cells (28), with sites other than Tyr-397 also being phosphorylated (25, 26), and most of the other tyrosine residues are phosphorylated by Src kinase *in vitro* (32). Similar to transformed cells, increased metastatic activity of prostate cancer cell lines correlates with increased pp125FAK expression and increased overall tyrosine phosphorylation (33). Therefore, it seems that tyrosine phosphorylation of pp125FAK participates in regulation of transformation in fibroblasts.

In the present study, we investigated the role of pp125FAK in detransformation using the HDAC inhibitor, TSA. Inhibition of HDAC activity down-regulates Src kinase activity, and in turn decreases phosphorylation of pp125FAK at Tyr-861. These changes, together with increased expression of several cytoskeletal proteins, result in spreading of Ha-*ras*-transformed NIH3T3 cells with a detransformed morphology. Therefore, TSA-induced detransformation correlates with decreased pp125FAK phosphorylation at tyrosine 861 in *ras*-transformed fibroblasts.

EXPERIMENTAL PROCEDURES

Reagents and Antibodies—Trichostatin A (4,6-dimethyl-7-[*p*-dimetylaminophenyl]-7-oxohepta-2,5-dienohydroxamic acid) was purchased from Sigma, and fibronectin (FN) was from Invitrogen. PP1 was from Calbiochem. Anti-phosphotyrosine (PY99), anti-RhoA (26C4), and anti-ERK2 (K-23) were from Santa Cruz Biotechnology, Inc. (Santa Cruz, CA). Anti-Src kinase antibody (GD11), anti-vinculin (V284), and anti-paxillin (5H11) were from Upstate Biotechnology, Inc. (Lake Placid, NY). Anti-α-actinin was from Sigma. Anti-integrin β_1 (clone 18) was from BD Pharmingen/Transduction Laboratories (San Diego, CA). Anti-pp125FAK and phosphorylation site-specific rabbit anti-pp125FAK p-Y397, p-Y407, p-Y576, p-Y577, p-Y861, and p-Y925 were from BIOSOURCE International, Inc. (Camarillo, CA).

Cell Lines and Cell Culture—NIH3T3, Ha-*ras*-NIH3T3, rat2, and K-*ras*-rat2 fibroblasts were maintained in Dulbecco's modified Eagle's medium supplemented with 10% fetal bovine serum, 10 units/ml penicillin, and 10 μg/ml streptomycin.

Cell Adhesion and Spreading Assays—Cell adhesion and spreading assays were performed on FN-coated tissue plates essentially as described (34). Briefly, FN was diluted in serum-free medium (SFM), added to tissue culture plates (final coating concentration, 2 $\mu g/cm^2$), and incubated at room temperature for at least 1 h to allow adsorption onto plates. After washing with phosphate-buffered saline, plates were blocked with 0.2% heat-inactivated bovine serum albumin for 1 h and then washed with SFM (2 × 10 min). While equilibrating SFM with FN-coated tissue culture plates at 37 °C and 10% CO_2, either TSA-treated or nontreated cells (final concentration 330 nM for 15 h) were detached with 0.05% trypsin, 0.53 mM EDTA; suspended in SFM containing 0.25 mg/ml soybean trypsin inhibitor; and centrifuged. Cells were resuspended in SFM and plated onto FN-coated plates and incubated for various periods of time at 37 °C. For cell morphology, cells were visualized with an inverted microscope (Zeiss, Germany) at ×20 magnification.

Immunoprecipitation and Immunoblotting—After cultures were washed twice with phosphate-buffered saline, the cells were lysed in RIPA buffer (50 mM Tris, pH 8.0, 150 mM NaCl, 1% Nonidet P-40, 0.1% SDS, 0.5% sodium deoxycholate, 10 mM NaF, 2 mM Na_3VO_4) containing a protease inhibitor mixture (1 μg/ml aprotinin, 1 μg/ml antipain, 5 μg/ml leupeptin, 1 μg/ml pepstatin A, 20 μg/ml phenylmethylsulfonyl fluoride). Cell lysates were clarified by centrifugation at 10,000 × *g* for 15 min at 4 °C, denatured with SDS-PAGE sample buffer, boiled, and analyzed by SDS-PAGE. For immunoprecipitations, each sample (containing 200–1000 μg of total protein) was incubated with the relevant antibody for 2 h at 4 °C; this was followed by the addition of protein G-Sepharose beads for 1 h. Immunoprecipitates were collected by centrifugation, washed three times with 1× RIPA buffer, resuspended in SDS sample buffer, boiled, and analyzed by SDS-PAGE. Proteins were transferred onto polyvinylidene difluoride membranes and probed with appropriate primary, followed by species-specific horseradish peroxidase-conjugated secondary antibodies. Signals were detected by enhanced chemiluminescence (ECL). The secondary antibodies, protein G-Sepharose beads, and ECL reagents were from Amersham Biosciences.

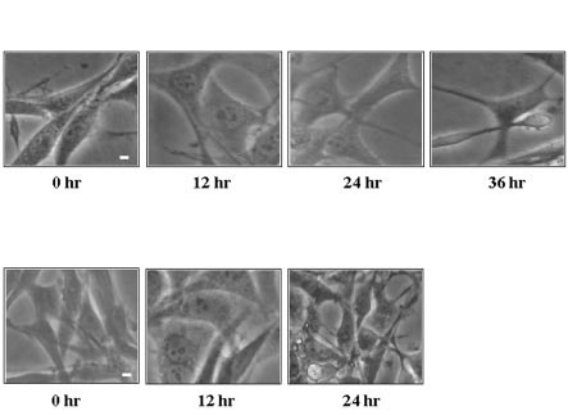

FIG. 1. **Inhibition of HDAC activity induces detransformation in fibroblasts.** Ha-*ras*-transformed NIH3T3 cells (*A*) and K-*ras*-transformed rat2 cells (*B*) were treated with TSA (330 nM) for the indicated time periods. The photograph was taken under phase-contrast optics with a digital camera. *Scale bars*, 10 μm.

pp125FAK Activity and Src Kinase Assays—For the pp125FAK activity assay, pp125FAK immunoprecipitates (containing 200 μg of total proteins, 1 μg of anti-pp125FAK antibody, and 20 μl of protein A-agarose beads) were washed with 1× RIPA buffer two times and with 10 mM Tris buffer one time. Pellets were dissolved in 20 μl of kinase buffer (10 mM Tris, pH 7.4, 10 mM $MnCl_2$, 2 mM $MgCl_2$, 0.02% Triton X-100), and reactions were started by adding 10 μCi of [γ-^{32}P]ATP, 1 μM cold ATP, and glutathione *S*-transferase-paxillin. The reactions were carried out at 25 °C for 5 min and adding 2× SDS-PAGE sample buffer. Samples were then analyzed by 8% SDS-PAGE and autoradiography.

For Src kinase assay, Src immunoprecipitates (containing 200 μg of total proteins, 1 μg of anti-Src antibody, and 20 μl of protein G-Sepharose beads) were washed with 1× RIPA two times and with 10 mM Tris buffer one time. Pellets were dissolved in 20 μl of kinase buffer (10 mM Tris, pH 7.4, 5 mM $MnCl_2$) and preincubated for 5 min at room temperature. The kinase reaction was started with the addition of 10 μCi of [γ-^{32}P]ATP, 1 μM cold ATP, and 2 μg of acid-denatured enolase. The reactions were carried out at room temperature for 5 min and adding 2× SDS-PAGE sample buffer. Samples were then analyzed by 8% SDS-PAGE and autoradiography.

Plasmids and Transfection—Insertion of c-Src cDNA into the pLNCX retroviral vector to construct pLNCX-c-Src and pLNCX vector were used. Transient transfections were carried out using LipofectAMINE reagent (Invitrogen) as described by the manufacturer. In brief, NIH3T3 cells were plated in 60-mm dishes and grown to ~80% confluence. The cells were transfected by adding 2 ml of a mixture of 15 μl of LipofectAMINE and 4 μg of the DNA plasmid to each culture dish. The cells were incubated in the above mixture for 5 h at 37 °C in a 5% CO_2, 95% air incubator. After the incubation, 2 ml of Dulbecco's modified Eagle's medium containing 10% fetal bovine serum was added to the transfection medium in each culture dish. Twenty-four hours later, the medium was aspirated and replaced with 2 ml of Dulbecco's modified Eagle's medium containing 10% fetal bovine serum.

RESULTS

Detransformation of ras-transformed Fibroblasts by TSA—Inhibition of HDAC activity is known to revert the phenotype of transformed cells (13, 14) into nontransformed phenotypes (2, 13, 14). Since the most clearly changed characteristic is an alteration of cytoskeletal organization, we investigated whether TSA regulates the functions of proteins involved in cytoskeletal organization. We confirmed the morphological changes by TSA in two different *ras*-transformed cells, Ha-*ras*-transformed NIH3T3 cells and K-*ras*-transformed rat2 cells after TSA treatment (Fig. 1). Similar to a previous report (35), 330 nM TSA induced a flattened and more spread morphology in both fibroblast lines, along with increased histone acetyla-

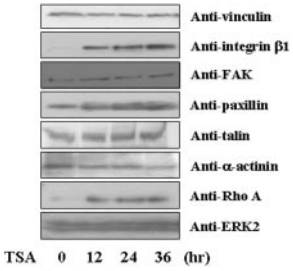

FIG. 2. **Inhibition of HDAC activity regulates expression of cytoskeletal proteins.** Ha-*ras*-transformed NIH3T3 cells were treated by TSA (330 nM) for the indicated periods of time. Total cell lysate (30 μg) was resolved by SDS-PAGE and subjected to immunoblotting with various antibodies recognizing cytoskeletal proteins. Antibodies are indicated.

tion (data not shown). The morphological changes in Ha-*ras*-transformed NIH3T3 cells were most pronounced after 24 h of TSA treatment (Fig. 1*A*) but at 12 h in K-*ras*-transformed rat2 cells (Fig. 1*B*).

Alteration of Cytoskeletal Protein Expression and Spreading on Fibronectin by TSA—Cell morphology is significantly dependent on the function of cytoskeletal proteins. Therefore, we investigated expression cytoskeletal protein of that might be involved in TSA-induced morphological changes. The most dramatic change was the induction of integrin β_1 adhesion receptor and cytosolic small G-protein RhoA (Fig. 2). Increased expression was detected at 12 h after TSA treatment and maintained over 36 h. On the other hand, the expression of paxillin was slightly increased, whereas other cytoskeletal proteins including vinculin, talin, α-actinin, and pp125FAK were unchanged. Since both integrin β_1 and RhoA are known as important regulators of ECM-mediated cytoskeletal organization (36), TSA-induced detransformation may be closely related with integrin-mediated adhesion to ECM. Spreading of Ha-*ras*-transformed and TSA-treated cells on fibronectin-coated plates was compared (Fig. 3). Detransformed cells attached and began to spread within 15 min and were completely spread within 30 min. Although Ha-*ras*-transformed NIH3T3 cells attached at the same rate as detransformed cells, a significant number of cells remained round at 15 min. Thus, compared with Ha-*ras*-transformed NIH3T3 cells, detransformed NIH3T3 cells showed faster spreading on fibronectin and maintained detransformed phenotypes.

Changed Tyrosine Phosphorylation of pp125FAK at Tyr-861—Tyrosine phosphorylation has been shown to be a common and ubiquitous response to integrin-ECM interaction (19, 22). Therefore, we investigated tyrosine phosphorylations after plating cells on fibronectin for 60 min (Fig. 4*A*). A dramatic change of tyrosine phosphorylation was detected on three different polypeptides, p130, p70, and p50. After incubation with TSA, tyrosine phosphorylation of p130 was increased, while that of p70 and p50 was decreased. Since pp125FAK is the major tyrosine-phosphorylated protein during cell-ECM interaction (24), we investigated whether p130 was pp125FAK using Western blotting and immunodepletion analysis (Fig. 4*B*). Phosphorylation of pp125FAK was decreased in *ras*-transformed NIH3T3 cells compared with NIH3T3 cells (*lanes 2* and *5*) but was partially restored by TSA treatment (*lanes 3* and *6*). After immunodepletion with a pp125FAK antibody, no pp125FAK was found in supernatant, confirming that p130 was pp125FAK. These observations suggest that TSA-induced morphological changes of Ha-*ras*-transformed NIH3T3 cells might be linked to the changed tyrosine phosphorylation and function of pp125FAK during spreading.

The functions of pp125FAK are regulated through specific tyrosine phosphorylation events, and six tyrosine phosphoacceptor sites have been identified (25, 26). We next examined the effect of TSA on each tyrosine phosphorylation site of pp125FAK during plating on fibronectin using phosphorylation site-specific antibodies. Analysis of Western blotting with total cell lysates or immunoprecipitates showed that TSA differentially regulated tyrosine phosphorylation of pp125FAK on the six tyrosine residues (Fig. 5*A*). Phosphorylation of the Tyr-397 autophosphorylation site was slightly increased, but there were no detectable changes at the Tyr-576 and Tyr-577 sites, implying unchanged kinase activity (25). Phosphorylation of Tyr-925 was too low to detect (data not shown). The most dramatic changes were found at Tyr-407 and Tyr-861. TSA-induced increased tyrosine phosphorylation at Tyr-407 and decreased tyrosine phosphorylation at Tyr-861, ~2.81 ± 0.73-fold (n = 3).

One explanation for the altered tyrosine phosphorylation was the alteration in spreading ability, which may not persist in long term events. To rule this out, exponentially growing

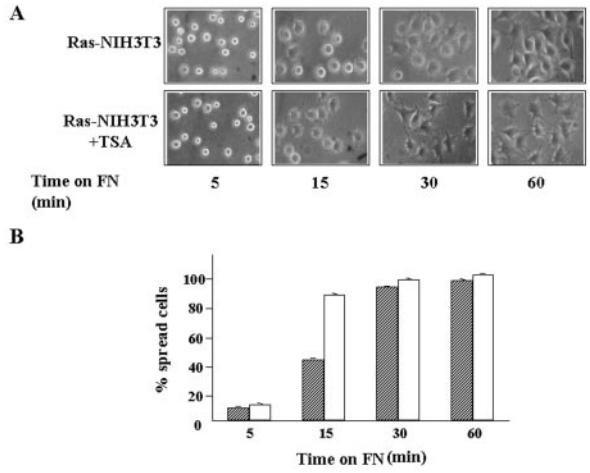

FIG. 3. **TSA-treated Ha-*ras*-transformed NIH3T3 cells exhibit enhanced spreading on fibronectin.** *A*, Ha-*ras*-transformed NIH3T3 cells and detransformed NIH3T3 cells were detached and replated on fibronectin-coated plates for the indicated time periods (in minutes), photographed under phase-contrast optics with a digital camera. *B*, quantification of the results of a spreading assay on fibronectin. The *black bar* shows Ha-*ras*-transformed NIH3T3 cells, and the *open bar* shows detransformed NIH3T3 cells. Values shown are the means ± S.E. of three independent experiments and are expressed as percentages of spread cells.

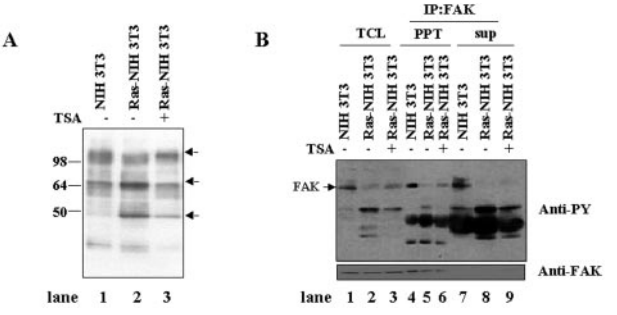

FIG. 4. **TSA induces increase in tyrosine phosphorylation on pp125FAK.** *A*, NIH3T3, Ha-*ras*-transformed NIH3T3, and TSA-treated cells were plated plated on fibronectin-coated plates for 60 min. Total cell lysate (30 μg) was resolved by SDS-PAGE and subjected to immunoblotting with anti-phosphotyrosine antibody. The *arrow* points to protein bands showing different phosphorylation. *B*, cells were plated for 60 min. Phosphorylated pp125FAK was analyzed by immunoprecipitation (*IP*) with anti-pp125FAK antibody followed by immunoblotting as described under "Experimental Procedures." Total cell lysates (*lanes 1–3*), pp125FAK immunoprecipitates (*PPT*; *lanes 4–6*), and supernatant after immunoprecipitation (*lanes 7–9*) were subjected to immunoblotting with anti-phosphotyrosine antibody (*upper panel*). Membranes were stripped and reprobed with anti-pp125FAK antibody (*lower panel*).

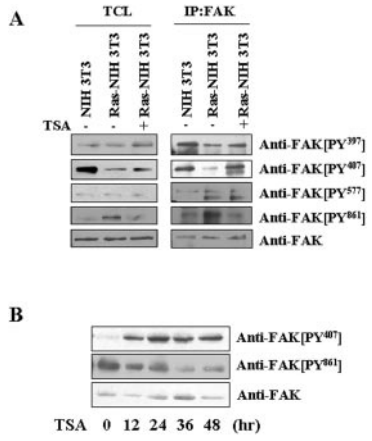

FIG. 5. **TSA induces increased Tyr-407 phosphorylation and decreased Tyr-861 phosphorylation on pp125FAK.** *A*, NIH3T3, Ha-*ras*-transformed NIH3T3, and TSA-treated cells were plated on fibronectin-coated plates for 60 min, and then total cell lysates (*left panel*) and pp125FAK immunoprecipitates (*right panel*) were resolved by SDS-PAGE. The site-specific phosphorylation of pp125FAK was analyzed by immunoblotting with anti-pp125FAK p-Y397, p-Y407, p-Y576, p-Y577, and p-Y861 antibodies. The amounts of proteins in immunoprecipitates were monitored by stripping and reblotting with anti-pp125FAK. *B*, Ha-*ras*-transformed NIH3T3 cells were incubated with TSA for the indicated periods of time. Phosphorylation of pp125FAK was analyzed as described above.

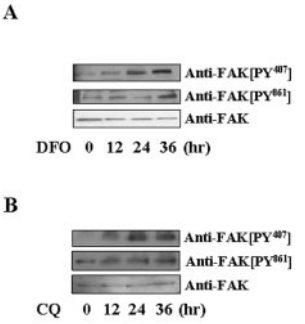

FIG. 6. **Cell cycle arrest affects pp125FAK phosphorylation at Tyr-407 but not at Tyr-861.** Ha-*ras*-transformed NIH3T3 cells were treated by either 20 μM deferoxamine (*DFO*; *A*) or 20 μM chloroquine (*CQ*; *B*) for the indicated periods of time. Phosphorylation of pp125FAK was analyzed as described in the legend to Fig. 5*A*.

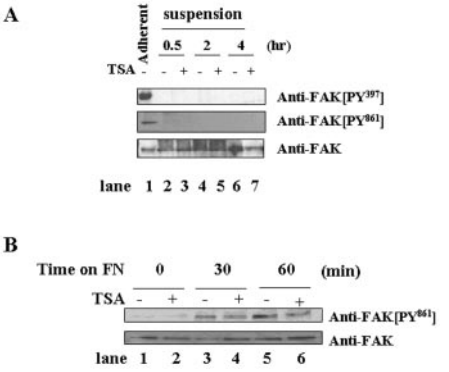

FIG. 7. **Tyr-861 phosphorylation on pp125FAK is dependent on adhesion.** Exponentially growing Ha-*ras*-transformed cells (−TSA) and detransformed cells (+TSA) were detached and either maintained in suspension (*A*) or replated on fibronectin-coated plates (*B*). After incubation for the indicated times, cells were lysed, and 30 μg of each lysate were used for immunoblotting with anti-pp125FAK p-Y397 (*upper panel*), p-Y861 (*middle panel*), or anti-pp125FAK (*lower panel*) antibody. For *lane 1* in *A*, exponentially growing Ha-*ras*-transformed cells were directly lysed.

Ha-*ras*-transformed cells were treated with TSA, and phosphorylation at Tyr-407 and Tyr-861 was investigated. Along with the morphological changes in Ha-*ras*-detransformed NIH3T3, phosphorylation at Tyr-407 was increased and phosphorylation at Tyr-861 was decreased in a time-dependent manner over 48 h (Fig. 5*B*). K-*ras*-transformed rat2 cells showed similar changes in tyrosine phosphorylation at Tyr-407 and Tyr-861 (data not shown).

Consistent with previous data (33), TSA induced cell cycle arrest in Ha-*ras* NIH3T3 cells (data not shown). Therefore, TSA may affect tyrosine phosphorylation of pp125FAK through cell cycle arrest. To test this, Ha-*ras*-detransformed NIH3T3 cells were treated with deferoxamine and chloroquine to arrest the cell cycle, and pp125FAK tyrosine phosphorylation was analyzed. Phosphorylation at Tyr-407 was increased, but phosphorylation at Tyr-861 remained unchanged (Fig. 6, *A* and *B*). These results indicate that decreased phosphorylation of Tyr-861 in pp125FAK correlates with the detransformation activity of TSA.

Adhesion-dependent Tyrosine Phosphorylation of Tyr-861—Tyrosine phosphorylations of pp125FAK may be involved in cytoskeletal organization during TSA-induced detransformation. It was possible that phosphorylation at Tyr-861 was dependent on cell-ECM adhesion. Two different approaches were used to test this hypothesis. Ha-*ras*-transformed cells were treated with TSA for 15 h, and cells were either lysed in RIPA buffer (Fig. 7A, *lane 1*) or trypsinized and maintained in suspension for up to 4 h (*lanes 2–7*). Following detachment, pp125FAK phosphorylation at Tyr-861 was decreased and was not detected in suspension cultured cells. However, when cells were replated onto fibronectin, pp125FAK phosphorylation at Tyr-861 was increased in a time-dependent manner (Fig. 7*B*). However, TSA-treated cells consistently showed 2 times less phosphorylation of Tyr-861 at 60 min postplating. These results demonstrate that pp125FAK phosphorylation at Tyr-861 is dependent on integrin-mediated adhesion.

Phosphorylation of pp125FAK at Tyr-861 Is Mediated by Src Family Kinases—It has been shown that pp125FAK Tyr-861 is phosphorylated by Src family kinases *in vitro* (25). To determine whether Src family kinases play a role in phosphorylation of pp125FAK at Tyr-861, we measured integrin-activated Src kinase activity in immunoprecipitates from both transformed and detransformed cells after plating on fibronectin (Fig. 8*A*). Integrin-activated Src kinase activity was much higher in *ras*-transformed cells than in TSA-treated cells. Since in many cases, the Src-pp125FAK complex is important in regulation of integrin-mediated cytoskeletal organization (22, 35), the activity of Src kinase interacting with pp125FAK was analyzed in pp125FAK immunoprecipitates (Fig. 8*B*). Src kinase activity in the immunoprecipitate was also decreased in TSA-treated cells. We further tested the effects of the Src family kinase inhibitor, PP1, on phosphorylation of pp125FAK at Tyr-861 in Ha-*ras*-transformed NIH3T3 cells (Fig. 8*C*). In the presence of 10 μM PP1, Tyr-861 phosphorylation was reduced substantially. Consistently, overexpression of Src kinase induced increased phosphorylation of pp125FAK at Tyr-861 (Fig. 8*D*). In addition, the amount of Src kinases present in pp125FAK immunoprecipitates was decreased in TSA-treated, detransformed cells (Fig. 9). All of these data suggest that Src kinase regulates phosphorylation of pp125FAK at Tyr-861, and decreased phosphorylation at Tyr-861 in TSA-treated detransformed cells is due to decreased Src family kinase activity and/or a decreased amount of Src kinase interacting with pp125FAK.

In contrast to Src family kinases, pp125FAK activity itself was not affected by TSA treatment (Fig. 10). *In vitro* kinase assays with pp125FAK immunoprecipitates and recombinant paxillin substrate showed that, even with decreased Tyr-861

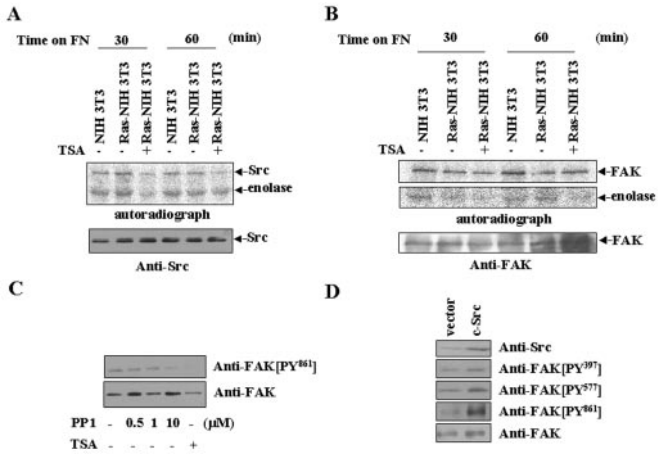

FIG. 8. **Src family kinases regulate phosphorylation at Tyr-861.** *A*, Src immunoprecipitates kinase assays were performed, with enolase as an exogenous substrate, on transformed or detransformed cells after plating on fibronectin at the times indicated. Autoradiography of phosphorylated Src and enolase are shown (*top panel*). The levels of Src present in each immunoprecipitate were determined by immunoblotting with anti-Src antibody (*bottom panel*). *B*, pp125FAK immunoprecipitate kinase assays were performed, with enolase as an exogenous substrate, on transformed or detransformed cells after plating on fibronectin at the times indicated. Autoradiography of phosphorylated pp125FAK and enolase are shown (*top panel*). The levels of pp125FAK present in each immunoprecipitate were determined by immunoblotting with anti-pp125FAK antibody (*bottom panel*). *C*, tyrosine phosphorylation at 861 in Ha-*ras*-NIH3T3 cells was blocked by PP1 treatment. Cells were treated with 0.5, 1, or 10 μM PP1 for 90 min, and 30 μg of each lysate were blotted for anti-pp125FAK p-Y397 (*upper panel*), p-Y861 (*middle panel*), or anti-pp125FAK (*lower panel*). *D*, c-Src cDNA was transiently transfected into NIH3T3 cells, and total cell lysates were prepared and immunoblotted for determination of tyrosine phosphorylation of pp125FAK as described above.

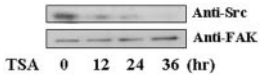

FIG. 9. **Association of Src kinase with pp125FAK is decreased in TSA-treated Ha-*ras*-transformed NIH3T3 cells.** Ha-*ras*-transformed NIH3T3 cells were treated by TSA (330 nM) for the indicated periods of time. Total cell lysates were used for immunoprecipitation with anti-pp125FAK. The levels of protein present in each immunoprecipitate were determined by immunoblotting with anti-Src antibody (*top panel*) and anti-pp125FAK (*bottom panel*).

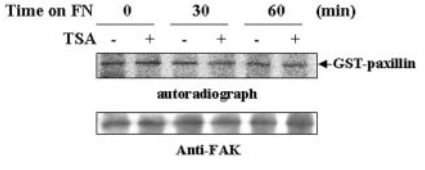

FIG. 10. **The activity of pp125FAK is not affected by TSA treatment.** pp125FAK immunoprecipitate kinase assays were performed, with recombinant paxillin as an exogenous substrate, on transformed or detransformed cells after plating on fibronectin as time indicated. Autoradiography of paxillin (glutathione *S*-transferase-paxillin (*GST-paxillin*)) is shown (*top panel*). The levels of pp125FAK present in each immunoprecipitates were determined by immunoblotting with anti-pp125FAK antibody (*bottom panel*).

phosphorylation, pp125FAK activity remained unchanged. Therefore, it seems that decreased Src kinase activity and phosphorylation at Tyr-861 are crucial for TSA-induced detransformation.

DISCUSSION

These studies show that Src family kinases are involved in Tyr-861 phosphorylation of pp125FAK, and this phosphorylation correlates with *ras*-induced transformation of fibroblasts. Inhibition of HDAC activity causes a decrease of Src activity and tyrosine phosphorylation of pp125FAK at Tyr-861, which results in detransformation of *ras*-transformed NIH3T3 fibroblasts.

In our experimental scheme, TSA-induced detransformation is coincident with changes in tyrosine phosphorylation of pp125FAK. Among six known phosphorylation sites in pp125FAK, the most dramatic change is decreased phosphorylation at Tyr-861. A relationship between Tyr-861 phosphorylation and transformation and/or tumorigenesis has been proposed, since 1) phosphorylation of pp125FAK at Tyr-861 is increased in Src-transformed fibroblasts (25, 26), and 2) increased phosphorylation of pp125FAK at Tyr-861 promotes increased cell migration in the highly tumorigenic prostate cell lines (33). Since decreased Tyr-861 phosphorylation of pp125FAK by TSA leads to a normal, detransformed morphology, this study strongly suggests that phosphorylation of pp125FAK at Tyr-861 is critical for the transformed morphology of fibroblasts.

The phosphorylation of pp125FAK at Tyr-861 is decreased by PP1, a Src family kinase inhibitor, and is increased by overexpression of c-Src (Fig. 8, *C* and *D*). Consistent with decreased phosphorylation at Tyr-861, TSA-treated fibroblasts show decreased Src kinase activity (Fig. 8*A*) and decreased interaction of Src kinase with pp125FAK (Fig. 9). Thus, it is likely that Src kinase is involved in phosphorylation of pp125FAK Tyr-861. However, we cannot exclude the possibility that other kinases exist, since the *in vitro* concentrations of PP1 that yield 50% inhibition for two major Src family tyrosine kinase in fibroblasts, Fyn and Src, are 6 and 170 nM, respectively (37), and a significant reduction of phosphorylation at Tyr-861 requires about 10 μM PP1.

How does HDAC activity regulate Src kinase activity? It is known that HDAC inhibitors increase the expression of gelsolin, a Ca^{2+}-dependent actin filament-severing and capping protein, by transcriptional activation of the gelsolin gene (38, 39). Thus, it may induce regulatory protein(s) that regulate Src kinase activity. Interestingly, HDAC inhibitor-induced morphological changes are suppressed by microinjection of anti-gelsolin antibodies, showing critical role of actin-associated proteins in cell morphological changes (38). In fact, TSA induces several different proteins, including integrin β1, RhoA, and paxillin (Fig. 2). Since Src kinase activity is dependent on cytoskeletal organization, it may also be possible that detransformed morphology regulates Src kinase activity.

At this point, it is unclear how increased tyrosine phosphorylation at Tyr-861 is associated with transformation of fibroblasts. It seems that the kinase activity of pp125FAK *per se* is not directly involved. Tyrosine phosphorylation of pp125FAK remains unchanged at tyrosines 576 and 577 (Fig. 5) and is required for its maximal kinase activity. Consistently, pp125FAK activity is not affected by TSA based on *in vitro* kinase assays (Fig. 10). The amount of pp125FAK remains unchanged after TSA treatment, implying that Tyr-861 phosphorylation is not involved in the stability of pp125FAK. Tyr-861 phosphorylation may be involved in interaction of pp125FAK with other signaling molecules and may create a new binding site to recruit SH2-containing signaling molecules that promote fibroblast transformation. Alternatively, this phosphorylation may regulate the interaction of pp125FAK with SH3 domain-containing proteins, since Tyr-861 is located in the middle of two proline-rich regions, PR1 and PR2. These regions are involved in interaction with SH3 domain-containing proteins such as Graf and $p130^{cas}$ (40, 41). Thus, it may interrupt the interaction of pp125FAK with SH3 domain-containing proteins, which negatively regulate transformation. Protein(s) specifically interacting with pp125FAK in trans-

formed cells will provide more clear answers on the relationship between pp125FAK phosphorylation and transformation.

Acknowledgments—We are grateful to Drs. Couchman and Woods for advice and critical reading of the manuscript.

REFERENCES

1. Spencer, V. A., and Davie, J. R. (2000) *J. Cell. Biochem. Suppl.* **35,** 27–35
2. Kwon, H. J., Owa, T., Hassig, C. A., Shimada, J., and Schreiber, S. L. (1998) *Proc. Natl. Acad. Sci. U. S. A.* **95,** 3356–3361
3. Zhong, Y., Delgado, Y., Gomez, J., Lee, S. W., Perez-Soler, R. (2001) *Clin. Cancer Res.* **7,** 1683–1687
4. Nakayama, S., Sasaki, A., Mese, H., Alcalde, R. E., Tsuji, T., and Matsumura, T. (2001) *Int. J. Cancer* **93,** 667–673
5. Sun, H., and Taneja, R. (2000) *Proc. Natl. Acad. Sci. U. S. A.* **97,** 4058–4063
6. Pazin, M. J., and Kadonaga, J. T. (1997) *Cell* **89,** 325–328
7. Knoepfler, P. S., and Eisenman, R. N. (1999) *Cell* **99,** 447–450
8. Ait-Si-Ali, S., Ramirez, S., Barre, F. X., Dkhissi, F., Magnaghi-Jaulin, L., Girault, J. A., Robin, P., Knibiehler, M., Pritchard, L. L., Ducommun, B., Trouche, D., and Harel-Bellan, A. (1998) *Nature* **396,** 184–186
9. Seo, S. B., McNamara, P., Heo, S., Turner, A., William, L. S., and Chakravarti, D. (2001) *Cell* **104,** 119–130
10. Hoshikawa, K., Kwon, H. J., Yoshida, M., Horinouchi, S., and Beppu, T. (1994) *Exp. Cell Res.* **214,** 189–197
11. Futamura, M., Monden, Y., Okabe, T., Fujita-Yoshigaki, J., and Yokoyama, S. Nishimura, S. (1995) *Oncogene* **10,** 1119–1123
12. Sugita, K., Koizumi, K., and Yoshida, H. (1992) *Cancer Res.* **52,** 168–172
13. Suzuki, T., Yokozaki, H., Kuniyasu, H., Hayashi, K., Naka, K., Ono, S., Ishikawa, T., Tahara, E., and Yasui, W. (2000) *Int. J. Cancer* **88,** 992–997
14. Vigushin, D. M., Ali, S., Pace, P. E., Mirsaidi, N., Ito, K., Adcock, I., and Coombes, R. C. (2001) *Clin. Cancer Res.* **7,** 971–976
15. Kapur, R., and Rudolph, A. S. (1998) *Exp. Cell Res.* **244,** 275–285
16. Hocking, D. C., Sottile, J., Reho, T., Fassler, R., and McKeown-Longo, P. J. (1999) *J. Biol. Chem.* **274,** 27257–27264
17. Brenner, K. A., Corbett, S. A., and Schwarzbauer, J. E. (2000) *Oncogene* **19,** 3156–3163
18. Hocking, D. C., Sottile, J., and Langenbach, K. J. (2000) *J. Biol. Chem.* **275,** 10673–10682
19. Burridge, K., and Chrzanowska-Wodnicka, M. (1996) *Annu. Rev. Cell Dev. Biol.* **12,** 463–519
20. Schoenwaelder, S. M., and Burridge, K. (1999) *Curr. Opin. Cell Biol.* **11,** 274–286
21. Aplin, A. E., and Juliano, R. L. (1999) *J. Cell Sci.* **112,** 695–705
22. Giancotti, F. G., and Ruoslahti, E. (1999) *Science* **285,** 1028–1032
23. Schaller, M. D., and Parsons, J. T. (1995) *Mol. Cell. Biol.* **15,** 2635–2645
24. Ilic, D., Damsky, C. H., and Yamamoto, T. (1997) *J. Cell Sci.* **110,** 401–407
25. Calalb, M. B., Zhang, X., Polte, T. R., and Hanks, S. K. (1996) *Biochem. Biophys. Res. Commun.* **228,** 662–668
26. Schlaepfer, D. D., Hanks, S. K., Hunter, T., and van der Geer, P. *(1994) Nature* **372,** 786–791
27. Schaller, M. D., Hildebrand, J. D., Shannon, J. D., Fox, J. W., Vines, R. R., and Parsons, J. T. (1994) *Mol. Cell. Biol.* **14,** 1680–1688
28. Guan, J. L., and Shalloway, D. (1992) *Nature* **358,** 690–692
29. Guinebault, C., Payrastre, B., Racaud-Sultan, C., Mazarguil, H., Breton, M., Mauco, G., Plantavid, M., and Chap, H. (1995) *J. Cell Biol.* **129,** 831–842
30. Calalb, M. B., Polte, T. R., and Hanks, S. K. (1995) *Mol. Cell. Biol.* **15,** 954–963
31. Sieg, D. J., Ilic, D., Jones, K. C., Damsky, C. H., Hunter, T., and Schlaepfer, D. D. (1998) *EMBO J.* **17,** 5933–5947
32. Owen, J. D., Ruest, P. J., Fry, D. W., and Hanks, S. K. (1999) *Mol. Cell. Biol.* **19,** 4806–4818
33. Slack, J. K., Adams, R. B., Rovin, J. D., Bissonette, E. A., Stoker, C. E., and Parsons, J. T. (2001) *Oncogene* **20,** 1152–1163
34. Woods, A., McCarthy, J. B., Furcht, L. T., and Couchman, J. R. (1993) *Mol. Biol. Cell* **4,** 605–613
35. Wharton, W., Savell, J., Cress, W. D., Seto, E., and Pledger, W. J. (2000) *J. Biol. Chem.* **275,** 33981–33987
36. Hotchin, N. A., and Hall, A. (1995) *J. Cell Biol.* **131,** 1857–1865
37. Hanke, J. H., Gardner, J. P., Dow, R. L., Changelian, P. S., Brissette, W. H., Weringer, E. J., Pollok, B. A., and Connelly, P. A. (1996) *J. Biol. Chem.* **271,** 695–701
38. Kwon, H. J., Yoshida, M., Nagaoka, R., Obinata, T., Beppu, T., and Horinouchi, S. (1997) *Oncogene* **15,** 2625–2631
39. Tanaka, M., Mullauer, L., Ogiso, Y., Fujita, H., Moriya, S., Fruuchi, K., Harabayashi, T., Shinohara, N., Koyanagi, T., and Kuzumaki, N. (1995) *Cancer Res.* **55,** 3228–3232
40. Hildebrand, J. D., Taylor, J. M., and Parsons, J. T. (1996) *Mol. Cell. Biol.* **16,** 3169–3178
41. Cary, L. A., Han, D. C., Polte, T. R., Hanks, S. K., and Guan, J. L. (1998) *J. Cell Biol.* **140,** 211–221

Trichostatin A-induced Detransformation Correlates with Decreased Focal Adhesion Kinase Phosphorylation at Tyrosine 861 in *ras*-transformed Fibroblasts

Yangmi Lim, Innoc Han, Ho Jeong Kwon and Eok-Soo Oh

J. Biol. Chem. 2002, 277:12735-12740.